THE JOURNAL OF PHYSICAL CHEMISTRY A

 VOLUME 108, NUMBER 49, DECEMBER 9, 2004

ARTICLES

50-fs Photoinduced Intramolecular Charge Separation in Triphenylmethane Lactones

Tanja Bizjak,[†] Jerzy Karpiuk,*[,‡] Stefan Lochbrunner,[†] and Eberhard Riedle*[,†]

Lehrstuhl für BioMolekulare Optik, Sektion Physik, Ludwig-Maximilians-Universität, Oettingenstrasse 67, 80538 München, Germany, and Institute of Physical Chemistry, Polish Academy of Sciences, Kasprzaka 44/52, 01-224 Warsaw, Poland

Received: June 17, 2004; In Final Form: September 21, 2004

Upon excitation of their structural subunits, phenolphthalein and malachite green lactone undergo ultrafast intramolecular charge separation with formation of a long-lived charge-transfer state (intramolecular "radical ion pair"). The kinetics of the primary charge separation in these molecules in aprotic solvents has been studied using femtosecond pump−probe spectroscopy. The phenol radical cation is formed by electron transfer within 50 fs after excitation of phenolphthalein to the S_1 state. In malachite green lactone the products of charge separation are observed 150 fs after excitation to the S_2 state. The results demonstrate that electron transfer in these molecules occurs faster than the time scale of inertial solvation dynamics. An intramolecular vibrational mode to promote charge separation is indicated.

1. Introduction

Photoinduced charge separation (CS) in donor−acceptor (D−A) systems is a fundamental photophysical process[1,2] that has attracted much attention particularly in view of its role in solar energy conversion and storage.[3] An ultrafast CS process ensures effective transformation of the energy of the absorbed photon into the energy of the emerging charge-transfer D^+-A^- state. With 6-fs electron transfer (ET) reported for strongly coupled dye/semiconductor colloidal systems[4] and even sub-3-fs charge-transfer time for biisonicotinic acid bound to a rutile TiO_2 surface, the research on heterogeneous CS has reached a very low femtosecond limit.[5] On the other hand, studies about *intramolecular* CS dynamics on the 100-fs time scale are very scarce. The reason is that the vast majority of investigated intramolecular ET processes are much slower than the time scale of molecular vibrations (e.g., due to an activation barrier), and in fact, they require vibrational assistance to proceed. In early work, diffusive solvation dynamics was shown to be a rate-limiting factor for many barrierless ET reactions in the condensed phase and the measured rate constants were correlated with the longitudinal dielectric relaxation time of the solvent (τ_L).[6,7] Further experimental studies have demonstrated that the rate of both intramolecular[8,9] and intermolecular[10,11] barrierless ET reactions can by far exceed τ_L and reach values as high as $k_{ET} = 10^{13}$ s^{-1}. This indicates that other factors such as ultrafast inertial solvation dynamics[12,13] or coupling of intramolecular vibrational modes[9,14] play critical roles in ET processes. The work on intramolecular CS dynamics occurring on the time scale of inertial solvation is still at the outset, and very few molecular systems have been found to be suitable for such studies. Recently, Nile blue linked to a 3-ferrocenophane group was shown to undergo ET within 90 fs,[15] and both ultrafast inertial solvation dynamics and intramolecular vibrational modes were found to promote the 80−100-fs ET process in a ruthenium mixed-valence compound in H_2O.[16] Somewhat slower CS (200 fs) was observed in porphyrinimide dyads[17] and in dimers of perylenediimide chlorophyll analogues (170 fs).[18] Very recently,

* To whom correspondence should be addressed. Fax: +49 89 2180 9202 (E.R.). E-mail: riedle@physik.uni-muenchen.de (E.R.); karpiuk@ichf.edu.pl (J.K.).
[†] Ludwig-Maximilians-Universität.
[‡] Polish Academy of Sciences.

10.1021/jp0473772 CCC: $27.50
Published on Web 11/11/2004

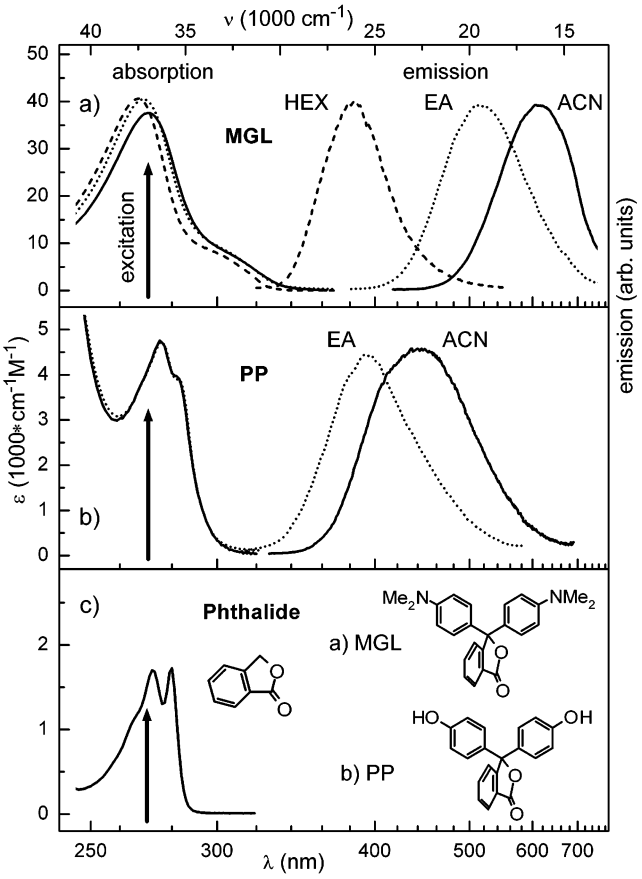

Figure 1. Steady-state absorption and emission spectra of (a) MGL, (b) PP, and (c) Pd in acetonitrile (solid line), ethyl acetate (dotted line), and *n*-hexane (dashed line). The shift of the emission spectrum increases with the solvent polarity. No fluorescence was found for phthalide. PP could not be dissolved in *n*-hexane. The excitation wavelength of 270 nm used in the femtosecond experiments is indicated in the spectra.

Kovalenko et al. proposed that the intrinsic ET process in cyanobianthryl proceeds within 10 fs.[19] A search for new D−A systems with extremely high ET rates and the exploration of known ones are very important both for practical reasons and for a deeper understanding of the various factors controlling the ET processes that occur on the time scale of vibrational relaxation, inertial solvation, or quantum dephasing.

A very promising class of molecules, in this context, are lactone forms of triarylmethane dyes (LTAM), relatively simple molecular systems with D and A units built around a tetrahedral carbon atom. Such an arrangement of D and A results in a weak electronic coupling in the ground state, and the absorption transitions in LTAMs in the lower energy region are localized on their structural subunits.[20] Despite such a weak coupling, the excitation of one of the dimethylaniline (DMA) groups in malachite green lactone (MGL; Figure 1) does not lead to any "local" fluorescence from DMA, but MGL rather displays a broad, strongly solvatochromic fluorescence band which has been ascribed to a highly polar CT state.[21] In contrast, structurally related leuco forms of malachite green with absorption spectra composed of the sum of their structural subunits,[22] in particular malachite green leuconitrile (MGCN), display only fluorescence from the primarily excited DMA moiety.[23] The absence of local fluorescence from the DMA moiety in MGL therefore indicates a rapid deactivation channel of the locally excited chromophore and has been ascribed to an ultrafast electron transfer from the excited DMA group to the phthalide (Pd) moiety. This assignment has been based on the analysis of steady-state fluorescence spectra of MGL and the photophysics of structurally related compounds.[21] Phenolphthalein (PP; Figure 1) is another LTAM which after excitation localized on one of its structural subunits displays fluorescence from a highly polar excited state populated upon electron transfer from one of the phenol rings to the Pd moiety.[24] Lack of fluorescence from the primarily excited structural subunit strongly indicates an ultrafast CS process also in the PP molecule.

In the present study the kinetics of charge separation in MGL and in PP in aprotic media have been directly measured with femtosecond pump−probe spectroscopy by monitoring the buildup of cation radicals of electron-donating moieties formed in the CS process. The cation radicals were identified with the help of transient spectra and the comparison to the nonreactive isolated Pd. Very short buildup times such as 50 fs for PP in acetonitrile show that the CS process occurs on the time scale of the inertial solvation dynamics and indicate a major role of a high-frequency intramolecular vibrational mode.

2. Experimental Section

MGL was synthesized as described by Fischer[25] and subsequently repeatedly recrystallized from 1-propanol. Commercially available PP (POCh; Polish Chemical Reagents S.A.) and Pd (Merck) were purified according to standard methods.[26] The solvents *n*-hexane (HEX), cyclohexane (CHEX), ethyl acetate (EA), and acetonitrile (ACN) were of spectroscopic quality. For fluorescence measurements, the optical densities of the samples were 0.1−0.15 at the excitation wavelengths. The concentrations of MGL, PP, and Pd in the laser experiments were chosen such that a typical transmission of a 0.12 mm free flowing jet was approximately 30%. Absorption spectra were recorded with a Perkin-Elmer Lambda 19 spectrophotometer, and the fluorescence spectra were measured with an Edinburgh Analytical Instruments FS900 spectrofluorometer. Fluorescence spectra were recorded as a function of wavelength and subsequently multiplied by a factor of λ^2 to convert counts per wavelength interval into counts per wavenumber interval. The fluorescence excitation spectra reproduce the absorption spectra well. The absorption spectra of MGL and PP did not change in laser measurements, which proves the photostability of both compounds under the experimental conditions used in this work.

Transient spectra were recorded with a white light continuum, and kinetic measurements were carried out with a two-color setup with 60-fs time resolution. A regenerative Ti:sapphire amplifier system (CPA 2001, Clark MXR) providing 150-fs pulses at 775 nm with a 1-kHz repetition rate was used to pump a two-stage noncollinear optical parametric amplifier (NOPA) that delivered 7−8-μJ pulses at 540 nm.[27,28] After precompression with a fused silica prism compressor, the pulses were focused by a 200-mm lens into a 110-μm-thick type I BBO crystal cut at 45°. Frequency-doubling of the overcompressed pulses yielded 1-μJ pulses at 270 nm with a duration of 50 fs without further compression. These pulses were used for the excitation of the investigated molecules in all experiments. A motorized translation stage was used to vary the time delay between the pump and probe pulses up to 1 ns.

A white light continuum was generated in a 2-mm-thick sapphire disk and was dispersed with an imaging grating spectrometer ($f = 20$ cm) after passing the sample. The chirp of the continuum, leading to a 320-fs delay between 435 and 730 nm, has not been corrected in the transient spectra, and the practical time resolution in measurements covering that wavelength region is conservatively estimated to be better than 1 ps. For two-color (kinetic) experiments, the probing pulse was generated by a single-stage NOPA tuned to 475 nm and

compressed to 30 fs with a fused silica prism sequence. The cross correlation measured by difference frequency generation in a 50-μm-thick BBO crystal was 60 fs. The excitation-induced transmission change of the sample was monitored by measuring the probe pulse energy after the sample with a photodiode on alternating laser shots with and without the excitation pulse. A part of the probe pulse was used as a reference beam to normalize for the fluctuations in laser intensity. The sample was a free flowing jet delivered by a sapphire nozzle with a 120-μm slit width, which assured that the excited volume was exchanged after each laser pulse. The data presented were normalized to pump pulse energy and sample concentration. The polarizations of the pump and probe pulses were set to the magic angle.

3. Results

3.1. Steady-State Absorption and Emission Spectra. Steady-state absorption and fluorescence spectra of MGL, PP, and Pd in solvents of different polarities are shown in Figure 1. The spectra do not show any absorption in the visible, indicating that only colorless lactone forms and no colored ionic forms (i.e., malachite green cation, MG^+,[29] or PP dianion, PP^{2-} [30]) were present in the solutions. Due to the orthogonal orientation of the structural subunits, the absorption spectrum of MGL above 250 nm is a superposition of the contributions from the DMA (actually 4-methyl-*N*,*N*′-dimethylaniline) and Pd moieties. No CT absorption transition can be identified.[21] At 270 nm, the Pd contribution to the MGL absorption is <5% (cf. molar absorption coefficients in Figure 1a,c), which means that predominantly the DMA groups are excited. The first absorption band of PP can also be considered as the sum of absorption transitions localized on the Pd moiety and on the phenol groups, and again no direct CT transition can be found in the spectrum.[24] Comparable molar absorption coefficients of phenol[31] and phthalide in the 250−290-nm region result in similar probabilities of excitation of each of these PP structural subunits with a 270-nm photon, so that not only local excitation of a phenol group but also that of the Pd moiety must be considered.

Both MGL and PP show a remarkable influence of the solvent polarity on the fluorescence spectra (Figure 1). The unusually large Stokes shift, strong solvatochromic effect, and large half-width of the fluorescence band indicate that the fluorescence in both molecules originates from a highly polar charge-transfer state. The dipole moments of the emitting state were determined from solvatochromic plots of the fluorescence maxima. The values of 25.0 and 21.0 D for MGL and PP, respectively, correspond to ET distances of 5.2 and 4.4 Å and suggest full electron transfer from the DMA group to the Pd moiety in MGL and from the phenol group to Pd in PP.[21,24] The absence of any fluorescence from the locally excited chromophore in both LTAMs (e.g., for MGL in ACN the upper limit for the quantum yield of such fluorescence is 3.6×10^{-6} [21]) could be well explained by a very fast conversion of the primarily excited FC state to the CT state due to intramolecular ET. In the case of MGL in ACN an upper limit for the transfer time of 130 fs was estimated earlier.[21] It should be noted that phenolphthalein has been generally perceived as a nonluminescent molecule, and except for two studies reporting very weak fluorescence from PP ionic forms in protic environments,[32,33] we are not aware of any luminescence studies on PP in aprotic media.

3.2. Transient Spectra: Radical Cation Signature. Transient absorption (TA) spectra were measured between 435 and 730 nm, where none of the molecules studied show ground-state absorption. The main contribution to the transient spectrum

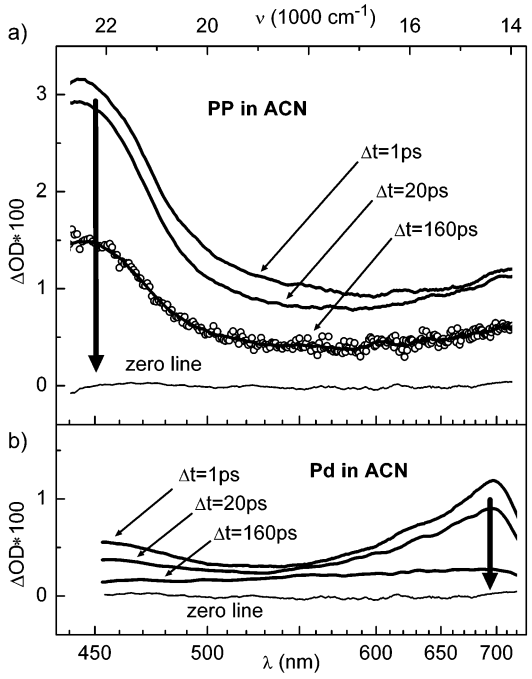

Figure 2. Time-dependent transient absorption recorded 1, 20, and 160 ps after 270-nm excitation of (a) PP in ACN and (b) Pd in ACN. Open circles are the data measured at a delay of 160 ps before smoothing over 10 points. The "zero line" (thin solid line) indicates the signal before the excitation. The transmissions of the PP and Pd solutions (120 μm jet) at 270 nm were 27% and 30%, respectively. The same excitation energy was used to record the spectra of both compounds. Note the different OD scales in (a) and (b).

of PP in ACN (Figure 2a) recorded 1 ps after excitation is a broad band with a maximum at 440 nm which decays exponentially with a decay time of 0.8 ns. The band can be ascribed neither to $S_n \leftarrow S_1$ absorption of phenol (maximum at 600 nm[34]) nor to $S_n \leftarrow S_1$ absorption of Pd, the other structural constituent of PP. To check the latter point, we also recorded the TA of Pd in ACN after 270-nm excitation. We found a weak TA band at 695 nm and a very weak one at 455 nm (Figure 2b); both bands decay simultaneously on a 50-ps time scale. The strong 440-nm band observed in the TA spectrum of PP matches very well the known absorption band of the phenol radical cation.[35] We therefore identify the observed spectral feature with the formation of a phenol radical cation in PP and consider its appearance in the TA spectrum at very small delay times as evidence that the photoinduced CS in PP is completed in less than 1 ps. We are not aware of any spectroscopic data on the phthalide radical anion (Pd^-), but the absence of other bands in the TA spectrum of PP in the wavelength region 500−700 nm indicates that its contribution to the TA spectra in the observed spectral range is weak.

The transient absorption spectrum of MGL in ACN recorded 1 ps after excitation to the S_2 state ($\lambda_{pump} = 270$ nm) shows a strong band at 465 nm that extends far to the red (Figure 3a) and decays exponentially with a decay time of 0.45 ns corresponding to the fluorescence decay time.[21] The shape of the TA spectrum matches the spectrum obtained in nanosecond measurements.[21] The dominant TA band at 465 nm cannot be assigned to $S_n \leftarrow S_1$ absorption of the DMA chromophore (peaking at 600−620 nm[36]) or to that of the Pd moiety (Figure 2b), but its position agrees with the absorption band of the dimethylaniline radical cation.[37] This indicates that the photoinduced CS in MGL is also completed within less than 1 ps.

Contrary to MGL dissolved in ACN, in EA the 465 nm band becomes narrower within the first few picoseconds while its

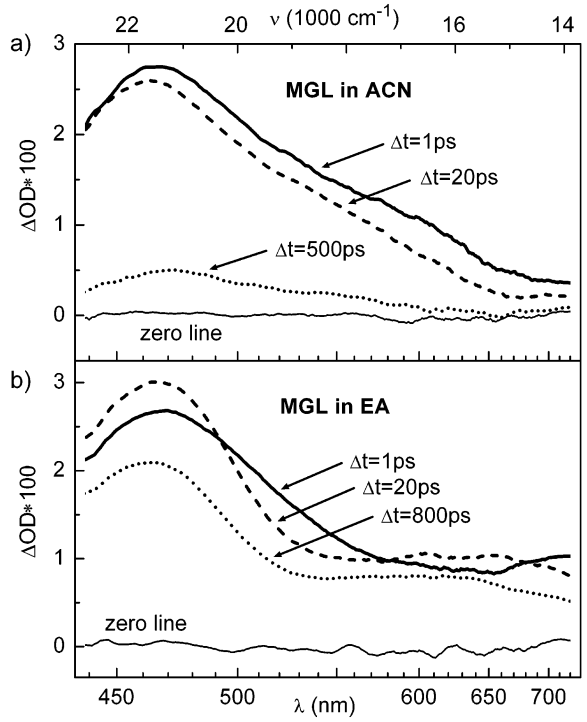

Figure 3. Transient absorption spectra of MGL in (a) ACN and (b) EA, recorded 1 ps (solid line), 20 ps (dashed line), and 800 ps (dotted line) after excitation at 270 nm. The zero line (thin solid line) indicates the signal before excitation. The transmissions of the MGL solution (120 μm jet) at 270 nm were 31% and 24% in ACN and in EA, respectively. The excitation energies were the same for both solvents.

maximum slightly increases (Figure 3b). This difference reflects the positions of the emission band in the two solvents (see Figure 1a) and the temporal evolution (red shift) of the emission spectrum of MGL in EA during diffusive solvation of the emerging CT state. The diffusive solvation times, τ_S, reported for ACN and EA are 0.4 and 2.6 ps, respectively,[38] and only for EA does our experiment resolve the diffusive solvation process. In ACN the emission band is far red detuned from the transient absorption and hardly influences the shape of the TA. In EA the emission band leads to a reduced absorption signal at probe wavelengths below 490 nm at early delay times and some picoseconds later to a dent of the absorption between 500 and 580 nm.

3.3. Two-Color Absorption Measurements: Ultrafast CS. The transient absorption spectra clearly document the appearance of CS products in PP and MGL, and their subsequent decay shows that the time of charge separation in both LTAMs studied is shorter than 1 ps. To determine the ET rate on the femtosecond time scale, the kinetics of the charge separation process were studied by recording the absorption buildup curves in the radical cation bands of PP and MGL. Figures 4 and 5 present early stages of the TA kinetic traces together with fitting curves. The latter were obtained by multiexponential (typically triexponential) fits assuming a Gaussian cross correlation with an fwhm equal to the experimentally determined value of 60 fs. Three time constants were necessary in the fit to account for (i) a rapid TA rise on the 50−200-fs time scale (τ_1), (ii) a slower low-amplitude TA rise or decay (depending on the solvent) observed in the 0.5−5-ps range (τ_2), and (iii) a long time decay (>400 ps) of the relaxed CT state (τ_3).

Figure 4 shows the buildup of the transient absorption at 475 nm for PP and Pd in ACN. The PP signal is best modeled with $\tau_1 = 0.05$ ps. Two curves simulating the absorption buildup of PP in ACN with $\tau_1 = 0.035$ ps and $\tau_1 = 0.070$ ps and all other

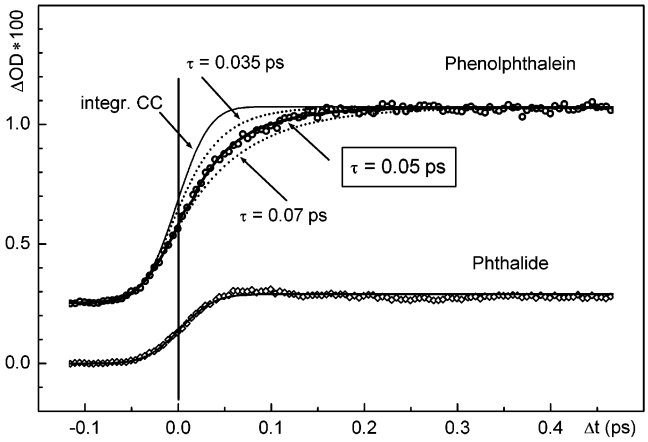

Figure 4. Transient absorption kinetic curves of PP and Pd in ACN recorded with probe pulses at 475 nm. A time constant of 50 fs was obtained from fitting the data (open symbols) with an exponential function (thick solid line, details in the text). Integrated cross correlation curves (thin lines) imitate the immediate appearance of TA to visualize the difference between a possible instantaneous buildup of TA and that with a finite time constant. The dotted lines are simulated TA buildups obtained with the same Gaussian excitation pulse but with time constants of 35 and 70 fs. The traces have been corrected for the solvent contribution and normalized for variations in the excitation energy.

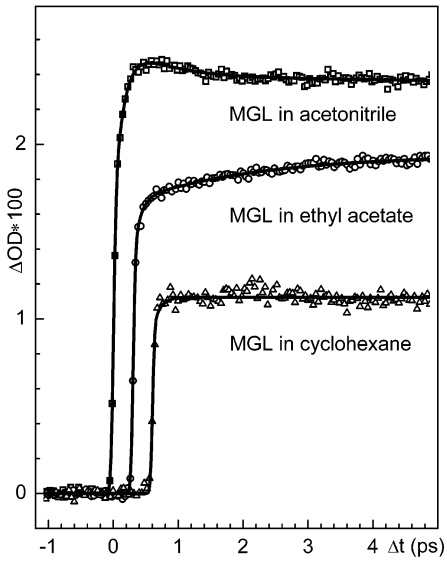

Figure 5. Transient absorption kinetic curves of MGL in ACN (squares), EA (circles), and CHEX (triangles) recorded with a probe pulse at 475 nm. For better visibility the latter two are shifted by 300 and 600 fs. The ultrafast rise of TA is followed by the diffusive solvation dynamics in polar solvents (ACN and EA). The transmissions of the MGL solutions (120 μm jet) at 270 nm were 36% in ACN, 26% in EA, and 51% in CHEX.

parameters kept constant are shown for comparison. In addition, the integrated experimental cross correlation curves are shown. They imitate the immediate appearance (0-fs rise time) of TA and demonstrate the difference between a hypothetical instantaneous buildup of TA and the finite time constant observed in the experiment for PP. From the comparison of all curves we can safely determine the ET time of PP in ACN to 50 ± 15 fs even though this time is slightly shorter than the experimental cross correlation. The buildup of the Pd transient absorption, both in ACN and in EA, corresponds very well to the integrated cross correlation, which means that the transient absorption of Pd appears immediately after excitation without any time delay measurable even on the femtosecond time scale. This observa-

TABLE 1: Time Constants Obtained from Fitting of Kinetic Curves[a]

molecule	solvent	τ_1 (ps)	A_1	τ_2 (ps)	A_2	τ_3 (ns)	A_3
PP	acetonitrile	0.05	−0.6	2.3	0.1	0.8	0.8
	ethyl acetate	0.08	−0.2	∼10	0.7	>2	0.7
MGL	acetonitrile	0.15	−0.7	0.65	0.2	0.45	1.5
	ethyl acetate	0.10	−0.2	2.5	−0.1	>2	1.1
	cyclohexane	≤0.10	−0.1			>2	0.7

[a] Negative amplitudes of the fitted constants indicate a rise component in transient absorption, positive amplitudes a decay.

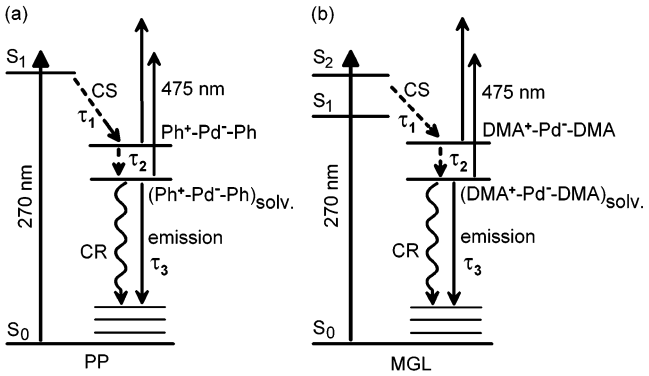

Figure 6. Energy scheme for ultrafast CS in PP (a) and MGL (b). See the text for details.

tion is in agreement with the expectation that no ET process or other ultrafast relaxation occurs in Pd.

For MGL in various solvents the initial time constant τ_1 is slightly longer and can be well resolved with the temporal resolution of our experiment (see Figure 5). In ACN and EA the amplitude of the second component is quite sizable for the detection wavelength of 475 nm and changes sign between ACN and EA. This is due to the differing strengths of the stimulated emission and excited-state absorption contributions that add to the overall transient absorption signal.

Both MGL and PP show a delayed absorption rise as compared to the integrated cross correlation (fitted with τ_1 time constants ranging from 50 to 150 fs), followed by a slower (τ_2 from subpicoseconds to several picoseconds) low-amplitude rise or decay which finally evolves into a long time decay of the relaxed CT state (τ_3). The time constants obtained from the fitting procedure are summarized in Table 1. PP was excited to its S_1 state; hence, the time constants of the TA rise in the phenol radical cation band (50 fs in ACN and 80 fs in EA) reflect the rate with which the product of the CS appears and therefore can be directly identified with the rate constants of the intramolecular ET process, $\tau_1 = \tau_{ET} = 1/k_{ET}$ (see Figure 6).

The somewhat longer rise times measured for MGL solutions in the DMA radical cation band (150 fs in ACN and 100 fs in EA) might reflect the fact that MGL was excited to the S_2 state (see Figures 1 and 6). If the $S_2 \rightarrow S_1$ vibronic relaxation precedes the ET, it could well delay the ET process by 10−100 fs,[39] and consequently the time until the DMA radical cation can be monitored (Figure 5). The intrinsic time of CS in MGL could be quite comparable to that found for PP, i.e., on the order of 50 fs. Alternatively, if the CS process proceeds directly from the S_2 state, the measured kinetics would show that the ET is somewhat slower in MGL than the extremely fast ET in PP. The transfer time of 100−150 fs would, however, still qualify MGL as one of the fastest known ET systems. Excitation to the S_1 state of MGL is needed to clarify which route is taken. Interestingly, MGL dissolved in cyclohexane shows a very fast TA buildup at 475 nm with $\tau_1 \leq 100$ fs,[40] indicating that the ET process in MGL occurs also in a nonpolar environment without any need for assistance from solvation. This observation is consistent with the broad and strongly Stokes shifted emission spectrum.

The slower overall CS time for MGL compared to PP seems surprising in view of the fact that more excess energy with respect to the CT state is deposited by the 270-nm optical excitation in MGL. From the extremely fast transfer in PP one might deduce that the process proceeds at the maximum of the Marcus parabola. An increased energy gap between the locally excited state and the CT state would lead to the inverted regime with a slightly reduced ET rate. This reduced vibrational overlap could explain the CS behavior of MGL. Additionally, we do not have any sound evidence whether the electronic coupling in MGL is as high as in PP. High-level quantum chemical calculations should allow the clarification of this point.

The values of the second time constant obtained from fitting (see τ_2 in Table 1) indicate their close relationship with diffusive solvation times reported for ACN and EA.[38] As discussed above (see section 3.2), the signal contributions with time constant τ_2 reflect the effect of the temporal evolution of the emission spectrum on the transient absorption spectrum during the diffusive solvation process of the emerging intramolecular CT state (see Figure 6). The small amplitudes of the τ_2 component indicate that the effect is rather insignificant at the wavelength of the radical cation observation (475 nm). This argument is supported by the absence of a τ_2 component in the nonpolar cyclohexane, where the fluorescence emitted at 475 nm is very weak. Finally, the long decays (τ_3 in Table 1 and Figure 6) represent the charge recombination (CR) process and the recovery of the ground-state population in both LTAMs studied.

4. Discussion

The overall structure of MGL and PP is quite similar and well-defined; they both have a nearly orthogonal arrangement of the electron-donating groups relative to the acceptor moiety. In PP the two phenol rings are twisted with respect to each other and form dihedral angles of 73.6° and 74.4° with the heterocyclic Pd ring and 72.9° with each other.[41] All C−C bonds of the central carbon atom (two with the phenols and one inside the lactone ring) are almost equally long, and their lengths (1.509−1.525 Å)[41] indicate that the delocalization of the electrons from the aromatic rings does not extend to the central C atom. A similar situation has been found for MGL.[21] The structural properties together with the fact that the low-energy absorption spectra of MGL and PP are a superposition of the spectra of their subunits allow us to conclude that the ground-state interactions between the structural components can be neglected in MGL and PP. The additivity of the spectra also shows that there are no direct optical CT absorption transitions in both LTAMs.[42] Such an electronic decoupling of structural components has also been found for another LTAM, crystal violet lactone,[20] and generally proven for spiropyrans[43] and various leuco forms of triarylmethanes, including malachite green leuconitrile.[22,23]

Upon excitation of their donor subunits, PP and MGL undergo ultrafast intramolecular charge separation with formation of a long-lived, highly polar ^{1}CT state as seen in our time-resolved measurements. The structure of the ^{1}CT state can be approximated as an intramolecular "radical ion pair" consisting of a radical cation of the electron donor and an anion radical of the electron acceptor (see Figure 6). These covalently bound structural subunits of the molecule subsequently undergo charge

recombination via emission and nonradiative decay to the ground state. The spectral signature of the DMA radical cation was already found in the nanosecond transient absorption spectra of MGL[21] and of the structurally similar crystal violet lactone,[20,44] where the limited time resolution allowed only the observation of the products of the photoinduced ET process. The emitting ^{1}CT state in MGL lies below the excited S_1 states of the individual structural subunits (DMA above 30200 cm^{-1} and Pd above 35700 cm^{-1} [21]) and is strongly stabilized by the interaction with the polar environment. The stabilization is reflected in the huge Stokes shift in highly polar solvents (exceeding, e.g., 16000 cm^{-1} for MGL in dimethyl sulfoxide).

The CS process in both LTAMs studied in this work is strongly exothermic and occurs in the nearly barrierless regime.[21,24] The free energy change, ΔG^0, in ACN was evaluated with the Weller equation[45] to be equal to -1.19 eV for MGL and -0.84 eV for PP. The value of ΔG^0 assumed earlier for MGL (-1.30 eV[21]) was corrected by using the reduction potential for phthalide from cyclic voltammetry measurements.[46] According to the two-dimensional ET model developed by Sumi and Marcus,[14] such a ΔG^0 value would result in ET reaction rates near the maximum of the "bell-shaped" curve ($\geq 7 \times 10^{12}$ s^{-1})[47] for the dependence of the ET rate on ΔG^0. This corresponds to the region where the sum of the free energy and the total reorganization energy λ is close to zero, and the ET processes are predicted to occur in a very low energy barrier or barrierless regime.

The fact that the time scale of the ET is faster than the diffusive solvation implies that the mutual orientation of the radical ions in the pair created by the ET must be very similar to that of the reactants during the ET process. In view of the well-defined donor−acceptor orientation in PP and MGL simple decay kinetics of the primarily excited chromophore and rise kinetics of the CS products can be expected and are indeed observed in the measurements. The ET dynamics is determined mainly by intramolecular vibrational motions and not by the orientational (diffusive) solvation process. This conclusion is strongly supported by the observation of an efficient CS process in MGL and PP in a nonpolar environment. No fluorescence from the locally excited state is found in these media, but instead CT luminescence with a large Stokes shift.

The very short times of radical cation formation presented above confirm our earlier estimate of τ_{ET}.[21] They provide clear evidence for an intramolecular ET process in LTAMs that occurs from a vibronically nonequilibrated level and is markedly faster than the diffusive solvation time scale. According to theories that model the dynamic solvation in ET reactions occurring under nonequilibrium conditions,[9,14,48,49] the ET rate and the trajectory along the reaction coordinate are determined by both the solvent relaxation rate (here the inertial dynamics component[13]) and the intramolecular degrees of freedom, which act as the ET promoting modes. The inertial solvation in ACN involves mainly small-amplitude rotational motions of solvent molecules in the first solvation shell, in particular the rotation of the cyanide group (−CN) around the CH_3−CN bond of the acetonitrile molecule.[50] It is now generally accepted that in many polar solvents (such as water or acetonitrile) about 60−70% of the solvation occurs in less than 100 fs.[12,49,51] The value of 50 fs determined for the ET time of PP in ACN excited to the S_1 state is the fastest intramolecular ET rate determined so far by a direct observation of ET product buildup kinetics. This value is also distinctly shorter than the 70-fs inertial component found in ACN ultrafast solvation dynamics[12] and lies below even longer times proposed for the inertial component in simulations of the ultrafast solvation dynamics of ACN.[50,51] If we take the 70-fs time constant as that describing the inertial solvation dynamics in ACN, we have to conclude that the photoinduced electron transfer in phenolphthalein in ACN occurs faster than the ballistic motions of the surrounding solvent molecules are able to stabilize the energy of the solute−solvent system. In addition, the observed effective and extremely fast ET in nonpolar environments suggests that polar solvation is not a precondition to reach the CT state. This in turn indicates a dominant role of high-frequency intramolecular vibrational modes in the CS process and negligible control by solvent dynamics. In LTAMs such a source of vibrational coupling is provided by the C−O bond in the lactonic ring, as electron capture by or transfer to the phthalide molecule results in excitation of C−O stretching vibrations, which leads to a C−O bond instability and a high probability for its cleavage.[46,52] In addition, the excess electronic energy resulting from electron capture by Pd was found to be preferably deposited in the C−O bond via a nuclear-excited Feshbach resonance.[52] The latter would indicate the possible formation of a dipole-bound Pd^- anion with an excess electron weakly bound by a long-range electrostatic field generated by the high dipole moment (4.9 D) of the Pd molecule[53] and residing on a very diffuse orbital outside the molecular frame.[54] Such an orbital might have significant overlap with the orbital of the primary excited donor part of the LTAM molecule, resulting in their coupling, which in turn would lead to the very high ET rates observed in these systems. A large spatial overlap of donor and acceptor orbitals has been found to be a prerequisite for an ultrafast ET.[55] Theoretical work is needed to explore the possibility of the occurrence and the electronic structure of dipole-bound resonance states involving Pd. Occupation of the diffuse orbital would correspond to the formation of a very short lived resonance state in the initial phase of the CS in LTAMs and might be of primary importance for a general understanding of the initial dynamics of CS processes in organic D−A systems.

5. Summary and Conclusions

Both LTAMs studied in this work, phenolphthalein and malachite green lactone, undergo ultrafast photoinduced CS with formation of a radical ion pair of their structural subunits. This observation confirms earlier predictions deduced from steady-state fluorescence spectra and from the analysis of structurally analogous compounds. The ET process was monitored directly with pump−probe femtosecond spectroscopy by measuring the kinetics of radical cation formation. In PP in ACN the phenol radical cation, a product of the primary CS, appears in the transient absorption spectra with a rise time of 50 fs. This is the fastest ET time constant directly observed so far for organic intramolecular D−A systems. The CS occurs on a time scale shorter than that postulated so far for ultrafast inertial solvation dynamics and is quite likely promoted by vibrational coupling to the C−O bond in the lactonic ring. The results prove the great suitability of LTAMs as model systems for both ultrafast ET and solvation dynamics studies. LTAMs are also excellent candidates for gaining insight into the detailed mechanisms of the very first stages of the electron-transfer process in organic D−A systems.

Acknowledgment. We thank Uli Schmidhammer and Vincent de Waele for valuable experimental assistance in setting up the broad-band transient absorption spectrometer. Financial support from Grant 3T09A05418 from the Committee of Scientific Research (KBN) and European Community Grant G5MA-CT-2002-04026 is gratefully acknowledged (J.K.). The

work was performed within the frame of the DFG Sonderforschungsbereich 377.

References and Notes

(1) Jortner, J.; Bixon, M., Eds. *Electron transfer: from isolated molecules to biomolecules*; Advances in Chemical Physics; J. Wiley: New York, 1999; Vols. 106 and 107.

(2) Balzani, V., et al., Eds. *Electron Transfer in Chemistry*; J. Wiley: New York, 2001.

(3) Fox, M. A., Channon M., Eds. *Photoinduced Electron Transfer*; Elsevier: Amsterdam, 1988.

(4) Huber, R.; Moser, J.-E.; Grätzel, M.; Wachtveitl, J. *J. Phys. Chem. B* **2002** *106*, 6494.

(5) Schnadt, J.; Brühwiler, P. A.; Patthey, L.; O'Shea, J. N.; Södergren, S.; Odelius, M.; Ahuja, R.; Karis, O.; Bässler, M.; Persson, P.; Siegbahn, H.; Lunell, S.; Mårtensson, N. *Nature* **2002**, *418*, 620.

(6) Zusman, L. D. *Chem. Phys.* **1980**, *49*, 295.

(7) Kosower, E. M.; Huppert, D. *Annu. Rev. Phys. Chem.* **1986**, *37*, 127.

(8) Pöllinger, F.; Heitele, H.; Michel-Beyerle, M. E.; Anders, C.; Fuscher, M.; Staab, H. A. *Chem. Phys. Lett.* **1992**, *198*, 645.

(9) Walker, G. C.; Åkesson, E.; Johnson, A. E.; Levinger, N. E.; Barbara, P. F. *J. Phys. Chem.* **1992**, *96*, 3728.

(10) Kobayashi, T.; Takagi, Y.; Kandori, H.; Kemnitz, K.; Yoshihara, K. *Chem. Phys. Lett.* **1991**, *180*, 416.

(11) Iwai, S.; Murata, S.; Tachiya, M. *J. Chem. Phys.* **1998**, *109*, 5963.

(12) Rosenthal, S. J.; Xie, X.; Du, M.; Fleming, G. R. *J. Chem. Phys.* **1991**, *95*, 4715.

(13) Maroncelli, M. *J. Mol. Liq.* **1993**, *57*, 1.

(14) Sumi, H.; Marcus, R. A. *J. Chem. Phys.* **1986**, *84*, 4894.

(15) Baigar, E.; Gilch, P.; Zinth, W.; Stöckl, M.; Härter, P.; von Feilitzsch, T.; Michel-Beyerle, M. E. *Chem. Phys. Lett.* **2002**, *352*, 176.

(16) Son, D. H.; Kambhampati, P.; Kee, T. W.; Barbara, P. F. *J. Phys. Chem. A* **2002**, *106*, 4591.

(17) Mataga, N.; Chosrowjan, H.; Taniguchi, S.; Shibata, Y.; Yoshida, N.; Osuka, A.; Kikuzawa, T.; Okada, T. *J. Phys. Chem. A* **2002**, *106*, 12191.

(18) Giaimo, J. M.; Gusev, A. V.; Wasielewski, M. R. *J. Am. Chem. Soc.* **2002**, *124*, 8530.

(19) Kovalenko, S. A.; Pérez Lustres, J. L.; Ernsting, N. P.; Rettig, W. *J. Phys. Chem. A* **2003**, *107*, 10228.

(20) Karpiuk, J. *J. Phys. Chem. A*, submitted for publication.

(21) Karpiuk, J. *Phys. Chem. Chem. Phys.* **2003**, *5*, 1078.

(22) Geiger, M. W.; Turro, N. J.; Waddell, W. H. *Photochem. Photobiol.* **1977**, *25*, 15. Sporer, A. H. *Trans. Faraday Soc.* **1961**, *57*, 983.

(23) Herz, M. L. *J. Am. Chem. Soc.* **1975**, *97*, 6777.

(24) Karpiuk, J. Manuscript in preparation.

(25) Fischer, O. *Justus Liebigs Ann. Chem.* **1881**, *206*, 83.

(26) Armarego, W. L. F.; Perrin, D. D. *Purification of Laboratory Chemicals*, 4th ed.; Butterworth-Heineman: Oxford, 1996.

(27) Wilhelm, T.; Piel, J.; Riedle, E. *Opt. Lett.* **1997**, *22*, 1494.

(28) Riedle, E.; Beutter, M.; Lochbrunner, S.; Piel, J.; Schenkl, S.; Spörlein, S.; Zinth, W. *Appl. Phys. B* **2000**, *71*, 457.

(29) Nagasawa, Y.; Ando, Y.; Kataoka, D.; Matsuda, H.; Miyasaka, H.; Okada, T. *J. Phys. Chem. A* **2002**, *106*, 2024.

(30) Tamura, Z.; Abe, S.; Ito, K.; Maeda, M. *Anal. Sci.* **1996**, *12*, 927.

(31) Berlmann, I. B. *Handbook of fluorescence spectra of aromatic molecules*; Academic Press: New York, 1971.

(32) Boguta, A.; Wróbel, D. *J. Fluoresc.* **2001**, *11*, 129.

(33) Gronowska, J.; Rakowska, T.; Waleryś, H. *Rocz. Chem.* **1973**, *47*, 2101.

(34) Hermann, R.; Mahalaxmi, G. R.; Jochum, T.; Naumov, S.; Brede, O. *J. Phys. Chem. A* **2002**, *106*, 2379.

(35) Hermann, R.; Naumov, S.; Mahalaxmi, G. R.; Brede, O. *Chem. Phys. Lett.* **2000**, *324*, 265.

(36) Oosterbaan, W. D.; Koeberg, M.; Piris, J.; Havenith, R. W. A.; van Walree, C. A.; Wegewijs, B. R.; Jenneskens, L. W.; Verhoeven, J. W. *J. Phys. Chem. A* **2001**, *105*, 5984.

(37) Shida, T.; Nosaka, Y.; Kato, T. *J. Phys. Chem.* **1978**, *82*, 695.

(38) Kahlow, M. A.; Kang, T. J.; Barbara, P. F. *J. Chem. Phys.* **1988**, *88*, 2372.

(39) Elsaesser, T.; Kaiser, W. *Annu. Rev. Phys. Chem.* **1991**, *42*, 83.

(40) Only this upper limit for the time constant in cyclohexane could be obtained due to uncertainities with a proper accounting for the solvent effect in the initial phase of the kinetic trace.

(41) Fitzgerald, L. J.; Gerkin, R. E. *Acta Crystallogr., C* **1998**, *54*, 535. Mean values of the angles reported for two crystallographically inequivalent PP molecules have been used.

(42) Detailed inspection of the low-energy region of the first absorption band of MGL in polar solvents revealed a very low intensity, nonvanishing tail with an estimated absorption coefficient of $<50\ M^{-1}\ cm^{-1}$ at 27800 cm^{-1}. Such a tail (with larger intensity) is clearly seen (at energies lower than 30000 cm^{-1}) in the MGL absorption spectrum published by Kuzuya et al.: Kuzuya, M.; Miyake, F.; Okuda, T. *Chem. Pharm. Bull.* **1983**, *31*, 791. Sample-dependent intensities of the tail and the fact that it has not been recovered in the fluorescence excitation spectra recorded in different solvents indicate that the absorption in this region is probably to be ascribed to impurity traces.

(43) Tyer, N. W., Jr.; Becker, R. S. *J. Am. Chem. Soc.* **1970**, *92*, 1289.

(44) Karpiuk, J. *Ann. Pol. Chem. Soc.* **2001**, 271.

(45) Rehm, D.; Weller, A. *Isr. J. Chem.* **1970**, *8*, 259.

(46) Vincent, M. L.; Peters, D. G. *J. Electroanal. Chem.* **1992**, *327*, 121.

(47) Nagasawa, Y.; Yartsev, A. P.; Tominaga, K.; Bisht, P. B.; Johnson, A. E.; Yoshihara, K. *J. Phys. Chem.* **1995**, *99*, 653.

(48) Jortner, J.; Bixon, M. *J. Chem. Phys.* **1988**, *88*, 167.

(49) Denny, R. A.; Bagchi, B.; Barbara, P. F. *J. Chem. Phys.* **2001**, *115*, 6058.

(50) Biswas, R.; Bagchi, B. *J. Phys. Chem. A* **1999**, *103*, 2495.

(51) Maroncelli, M. *J. Chem. Phys.* **1991**, *94*, 2084.

(52) Zykov, B. G.; Vasil'ev, Y. V.; Fal'ko, V. S.; Lachinov, A. N.; Khvostenko V. I.; Gileva, N. G. *JETP Lett.* **1996**, *64*, 439.

(53) Wallmark, I.; Krackov, M. H.; Chu, S.-H.; Mautner, H. G. *J. Am. Chem. Soc.* **1970**, *92*, 4447.

(54) Desfrançois, C.; Abdoul-Carime, H.; Schermann, J.-P. *Int. J. Mod. Phys. B* **1996**, *10*, 1339.

(55) Fiebig, T.; Stock, K.; Lochbrunner, S.; Riedle, E. *Chem. Phys. Lett.* **2001**, *345*, 81.